Experimental Study of the QCD Phase Diagram and Search for the Critical Point: Selected Arguments for the Run-10 Beam Energy Scan at RHIC

The STAR Collaboration (B. I. Abelev et al.)

Introduction & Summary

We present an overview of the main ideas that have emerged from discussions within STAR for the Beam Energy Scan (BES). The formulation of this concise and abridged document is facilitated by the existence of a much longer and more comprehensive companion document entitled *Experimental Exploration of the QCD Phase Diagram: Search for the Critical Point* [1]. The compelling arguments and motivations for the physics of our proposed Beam Energy Scan program, which have a particular role in guiding the run plan (see p. 13) as set out in our discussion of Tables 1 and 2, are (not in order of priority):

A. A search for turn-off of new phenomena already established at higher RHIC energies; QGP signatures are the most obvious example, but we define this category more broadly. If our current understanding of RHIC physics and these signatures is correct, a turn-off must be observed in several signatures, and such corroboration is an essential part of the "unfinished business" of QGP discovery [2]. The particular observables that STAR has identified as the essential drivers of our run plan are:
   - (A-1) Constituent-quark-number scaling of v_2 , indicating partonic degrees of freedom;
   - (A-2) Hadron suppression in central collisions as characterized by the ratio R_{CP} ;
   - (A-3) Untriggered pair correlations in the space of pair separation in azimuth and pseudorapidity, which elucidate the ridge phenomenon;
   - (A-4) Local parity violation in strong interactions, an emerging and important RHIC discovery in its own right, is generally believed to require deconfinement, and thus also is expected to turn-off at lower energies.

B. A search for signatures of a phase transition and a critical point. The particular observables that we have identified as the essential drivers of our run plan are:
   - (B-1) Elliptic & directed flow for charged particles and for identified protons and pions, which have been identified by many theorists as highly promising indicators of a "softest point" in the nuclear equation of state;
   - (B-2) Azimuthally-sensitive femtoscopy, which adds to the standard HBT observables by allowing the tilt angle of the ellipsoid-like particle source in coordinate space to be measured; these measurements hold promise for identifying a softest point, and complements the momentum-space information revealed by flow measurements, and
   - (B-3) Fluctuation measures, indicated by large jumps in the baryon, charge and strangeness susceptibilities, as a function of system temperature – the most obvious expected manifestation of critical phenomena.

Approaching the proposed BES program with the realization that a lesson from the past history of relativistic heavy-ion physics is to expect surprises, we offer a physics vision that is presented in Table 2 (page 14), in which we emphasize the highly diverse analysis options made possible by the large acceptance and general-purpose capabilities of the STAR detector, especially with the enhanced particle ID capabilities added by the full Time-of-Flight barrel coming online in Run-10. Table 2 is a concise illustration that STAR is highly adaptable and flexible, and we are ready to find and characterize the almost-inevitable surprises that will be in store as we explore the new frontier of the BES.

Recent analyses of a few thousand Au + Au events at $\sqrt{s_{\mathrm{NN}}}$ = 9.2 GeV, recorded during a short beam development test in spring 2008, provide ample evidence that the STAR detector is fully ready and capable of successful operation at sub-injection energies.

Many factors constrain our planning for BES running at STAR. These include the upcoming Heavy Flavor Tracker and Forward GEM Tracker subsystems, which will impact the future availability of one or both Forward Time Projection Chambers (FTPC) – proven existing subsystems that provide information about the reaction plane needed for measuring the v_1 component of flow and considerably extend pseudorapidity coverage. New 4-cm-diameter beam pipes are also coming to both PHENIX and STAR in Run-11. The implication for BES of these new pipes is still under study, but there is a danger of very serious degradation of RHIC performance at low beam energies. Therefore, we view Run-10 as a unique opportunity for an exploratory Energy Scan.

The QCD Phase Diagram

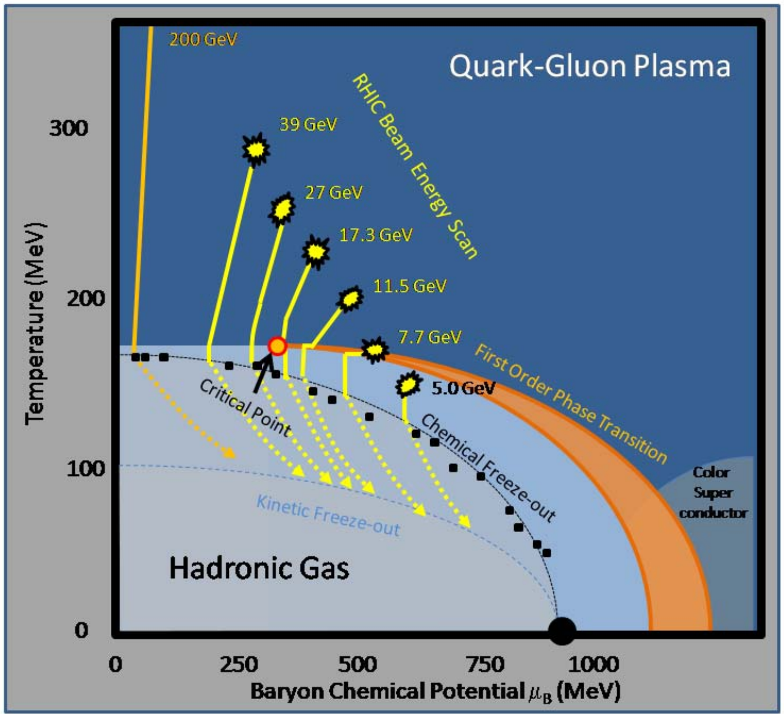

Fig. 1: A schematic representation of the QCD Phase Diagram. The location of the critical point, the separation between the 1st-order transition and chemical freeze-out, and the focusing of the event trajectories towards the critical point, are not based on specific quantitative predictions, but are all chosen to illustrate plausible possibilities.

The QCD phase diagram, schematically sketched in Fig. 1, lies at the heart of what the RHIC Physics Program is all about. It contains information about the location of phase boundaries (the phase transition is indicated by the orange band) and the physics of the phases, hadronic gas (HG, light blue) and quark-gluon plasma (QGP, navy), that are separated by this boundary.

So far, our understanding of this diagram is limited to the "edges" [7]: Lattice QCD calculations at vanishing chemical potential μ_B indicate a rapid, but smooth cross-over transition at a large temperature T [3], while various models representing matter at vanishing T predict a strong first-order phase transition at a large μ_B [4]. If both classes of models are correct, then a critical point (marked by the red circle in Fig.1) must be located where the transition changes from a smooth cross-over to first-order [5]. Exploring the rest of the QCD phase diagram ($T \neq 0$ and $\mu_B \neq 0$) presents a formidable challenge. Several methods have been applied to lattice QCD to overcome existing numerical problems at non-vanishing μ_B, but there is no agreement in the predictions of the location, or even the existence, of the critical point so far. An additional complication comes from the fact that the systematic errors of lattice calculations are neither understood nor constrained.

Given the very significant theoretical difficulties, it falls to the experiments to resolve the questions. The BES experimental program at RHIC with heavy ion collisions at energies in the range $\sqrt{s_{\mathrm{NN}}}$ = 5 to 39 GeV is designed to provide observational evidence for the existence of the critical point and to explore the unknown "territories" of the QCD phase diagram. Heavy ion collisions provide a unique experimental opportunity for such exploration; by varying the center-of-mass energy of the colliding nuclei, one can access different values of μ_B (collisions with higher energies probe lower μ_B values). The yellow lines in Fig. 1 represent reaction trajectories at energies proposed for the first run of the BES program (from right to left: $\sqrt{s_{\mathrm{NN}}}$ = 5, 7.7, 11.5, 17.3, 27 and 39 GeV). While stepping in μ_B, one needs to pay close attention to many observables, in particular the signatures predicted for phase transition and the critical point. A non-monotonic dependence of variables on $\sqrt{s_{\mathrm{NN}}}$ and an increase of long-wavelength fluctuations should become apparent only near the critical point. The rise and then fall of this signal as μ_B increases should allow us to ascertain the (T, μ_B) coordinates of the critical point. The onset of the non-equilibrium “lumpy” final state is expected after cooling through a first-order phase transition. Those fluctuations will have non-Gaussian character.

Note that the magnitude of these non-monotonic excursions, as well as the probability that they will survive the final state interactions, is difficult to predict. Fortunately for the experiments, there may not be a need for a trajectory to “pass” precisely through the critical point in the (T, μ_B) plane to see the signatures, as some hydrodynamic calculations show that the critical point “attracts” trajectories [6]. In such a case, if the trajectory misses the critical point by a few tens of MeV along the μ_B axis, the signature will be just as strong as if it were to pass directly through it. Note, however, that this “attraction” is not generic, and relies on specific features of the EOS near the critical point [6]. The exact position of the critical point in Fig.1, as well as the associated attraction of trajectories, was chosen for illustration purposes only [6]. Although subsequent running can use smaller steps in μ_B to verify and trace the possible effect of focusing and to pin down the critical point, the first exploration of unknown territories of (T, μ_B) space will be done with a few steps in $\sqrt{s_{NN}}$ to narrow down an area of interest for further study (see Table 1 on p.13).

Establishing the existence of the critical point, or the existence of both a cross-over and a first/second order transition, would surely place RHIC results into textbooks around the world.

A. Turn-off of QGP Signatures and Other New Phenomena

(A-1) Constituent-quark-number scaling

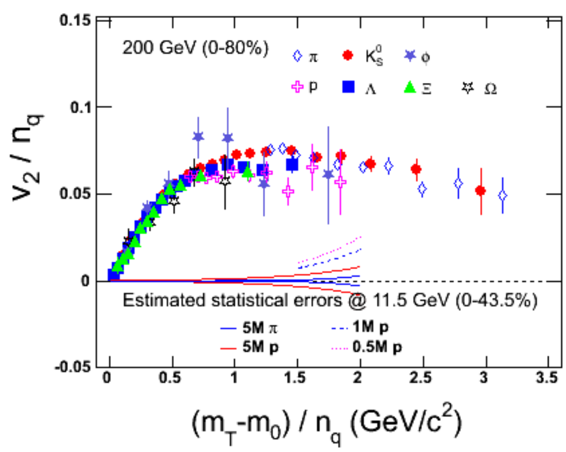

Fig. 2: Elliptic flow per constituent quark versus transverse mass per constituent quark for Au + Au collisions at 200 GeV at RHIC. See text for explanation of solid and dashed curves near v_2 = 0.

When elliptic flow v_2 is plotted versus transverse kinetic energy ($m_T - m_0$), v_2 for all identified particles below $m_T - m_0$ = 0.9 GeV/c^2 falls on a universal curve. Above that, meson and baryon v_2 deviates, with baryon v_2 rising above meson v_2 and saturating at a value approximately 50% larger than for mesons; however, upon dividing each axis by the number of constituent quarks (n_q = 2 for mesons and 3 for baryons), the meson and baryon curves merge very impressively into a single curve over a wide range of $m_T - m_0$, as seen in Fig. 2. This well-known scaling behavior is one of the most striking pieces of evidence for the existence of partonic degrees of freedom during the Au + Au collision process at 200 GeV. It is very hard to explain this pattern in a scenario where only hadronic matter exists throughout the interaction, whereas the hypothesis of coalescence of hadrons from deconfined quarks offers a ready explanation.

An observation of this n_q scaling behavior turning off below some threshold beam energy would be a very powerful confirmation of our current understanding of the deconfined phase. The ($m_T - m_0$)/n_q reach of the NA49 data at the top SPS energy is only 0.9 GeV/c^2 [8]. Data in this range does not test quark number scaling and is therefore not sufficient to answer the question of whether a similar v_2/n_q-scaling extends to lower beam energies. Extending the n_q scaling studies to BES energies, with a reach to 2.0 GeV/c^2 should provide a definitive answer to this question.

The solid and dashed curves in Fig. 2 near v_2 = 0 show the simulated magnitude of v_2/n_q error bars in the scenario of running Au + Au at $\sqrt{s_{NN}}$ = 11.5 GeV with the full ToF barrel in operation. With 5 million events, error bars are very small on protons, and even smaller on pions. The dotted line illustrate that even with just a half-million events, we would still have a reduced but probably adequate ability to compare pions and protons, and thereby test if the scaling still holds. Table 2 (page 14) includes additional information about the energy dependence of STAR’s simulated performance for this hallmark observable, including our capabilities for heavier mesons and baryons. Elliptic flow measurements for φ and Ω, particles that have relatively low hadronic interaction cross sections and are more promising probes of the early stages of the collision, open the door to testing partonic collectivity with improved confidence [52]. For testing π, K, p and Λ up to $(m_T - m_0)/n_q \sim 2$ GeV/c^2 with strong statistical significance, we need on the order of 5 million events at each BES energy point, whereas for ϕ and Ω, the statistical requirement become prohibitive below injection energy. In summary, we are confident that STAR has some capability to search for the crucial turn-off of n_q scaling at all BES energies where on the order of a million events are collected, as illustrated by Fig. 2.

(A-2) High & Intermediate p_T Spectra: QGP Opacity and the Baryon Anomaly

Hadron suppression through jet quenching has been a key observable for estimating the density of the matter created in heavy-ion collisions. In 200 GeV Au+Au collisions, high p_T hadron yields are suppressed by a factor of five relative to N_{binary}-scaled p+p collisions. In 22.4 GeV Cu+Cu collisions, however, neutral pion yields at p_T = 4 GeV/c are enhanced by a factor of 2. Such a behavior is characteristic of lighter systems (the number of participants is about a factor 3 lower in Cu+Cu than in Au+Au). This conclusion is not yet firm, however, because the p_T-reach of the 22.4 GeV Cu+Cu measurements extends only to 4 GeV/c. In this momentum range, the baryon to meson ratio is enhanced. In 62.4 GeV Au+Au collisions, the suppression is similar to that at 200 GeV, indicating that the strong jet quenching seen at top RHIC energies may set in somewhere below 62.4 GeV. A similar degree of suppression is observed also in Pb+Pb collisions at 17.3 GeV. The two CERN experiments NA49 [47] and WA98 [48] report $R_{AA} < 1$ up to p_T of 3.5 GeV/c, which indicates that suppression may set in at even lower energies, below 17.3 GeV. The particle type dependence of the nuclear modification factor R_{CP} shows a dependence on constituent quark number rather than mass, indicating that baryon yields increase faster with the matter density than meson yields. This dependence, coupled with the quark number scaling observed in v_2, suggests that fragmentation does not dominate hadron production here, but rather some multi-quark or gluon process and/or flow.
Measurements of the baryon to meson ratios and identified particle R_{CP} for p_T up to and above 4.5 GeV/c in the $\sqrt{s_{NN}}$ range between 17.3 and 62.4 GeV will allow STAR to disentangle effects that appear to dominate the intermediate p_T region. This is required to infer whether there is an onset of QGP opacity between 17.3 GeV and 62.4 GeV. At beam energies above 28 GeV, the R_{CP} and baryon-to-meson ratio studies can be bolstered with studies of the jet cone through triggered di-hadron correlations.

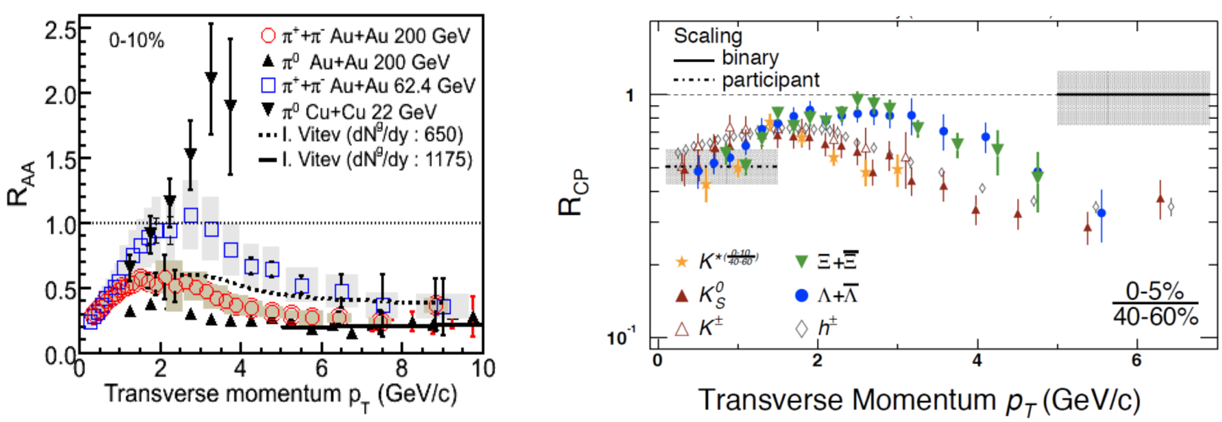

Fig. 3: The left panel shows STAR measurements of charged pion R_{AA} in Au+Au collisions at 62.4 and 200 GeV, and PHENIX measurements of neutral pion R_{AA} in Au+Au at 200 GeV, and in Cu+Cu at 22.4 GeV. The 22.4 GeV data are based on 6 million collisions. The right panel shows STAR measurements of identified particle R_{CP} in 200 GeV Au+Au collisions. Baryons are less suppressed than mesons. At intermediate p_T, all baryons lie in one group above the mesons.

The number of events required for high-p_T di-hadron studies was estimated based on PYTHIA. The estimates depend strongly on the p_T of the trigger and associated particle. For the high p_T spectra studies at 17.3 GeV, we base our estimates on existing measurements from NA49 and PHENIX. PHENIX measured neutral pion R_{AA} up to p_T = 4 GeV/c with 6 million 22.4 GeV Cu+Cu collisions. NA49 measured identified particle spectra up to p_T = 4.5 GeV/c with 800 thousand central 17.3 GeV Pb+Pb collisions. The acceptance of the STAR detector is roughly a factor of 1.8 larger than NA49 (-0.3<y<0.7 vs. 0.9<y<0.9) and a factor of 5 larger than PHENIX. We are confident therefore that 15 million minimum bias Au+Au collisions at 17.3 GeV will allow STAR to measure R_{CP} up to p_T = 4.5 GeV/c, where it is believed that fragmentation begins to dominate particle yields. Samples of 33 and 24 million events at 28 and 39 GeV will provide enough statistics to reach p_T values of 5 and 5.5 GeV/c, respectively, and will also provide the statistics needed to resolve the jet cone using triggered di-hadron correlations. These data sets will therefore allow STAR to perform definitive tests for an onset of QGP opacity and to test models for multi-quark and gluon hadron production, such as the recombination and coalescence models. The energy dependence of the baryon to meson ratio will be a particularly stringent test of models that rely on the interplay between a falling p_T spectrum and recombination or flow to describe the baryon enhancement.

(A-3) Pair Correlations in the Space of Pair Separation in Azimuth and Pseudorapidity

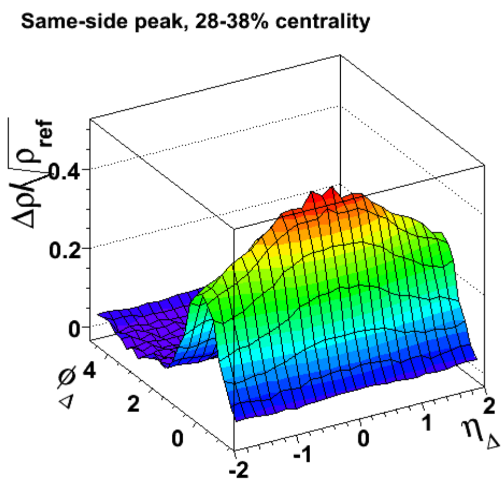

Fig. 4: Pair correlations for 200 GeV Au+Au as a function of pair separation in azimuth and pseudorapidity, after subtracting elliptic flow and an unrelated enhancement in the region where both differences are very small.

STAR's broad and uniform acceptance in both azimuth and pseudorapidity make it the ideal detector to reveal the full structure of many classes of correlation. The quantity $\Delta\rho/\sqrt{\rho_{ref}}$ plotted in Fig. 4 is constructed from the number of particle pairs separated by ϕ_Δ in azimuth and η_Δ in pseudorapidity. ρ_{ref} is a mixed-event reference, and $\Delta\rho$ is the number of real pairs minus ρ_{ref} [15]. This type of observable is sensitive to the familiar cos 2ϕ modulation arising from elliptic flow, but this flow has already been subtracted in Fig. 4. A spike at (0, 0) due to photon conversions and HBT has also been subtracted; what remains is a correlation strongly elongated in η_Δ at small ϕ_Δ known as the "ridge". This structure is fit quite well with a 2D Gaussian, and Fig. 5 provides further details about the parameters of this Gaussian as a function of the centrality measure ν. The most striking feature of the ridge is its steep increase in both amplitude and pseudorapidity width as collision centrality increases. Over the same centrality range, the width along the ϕ axis decreases slightly, and the behavior is qualitatively similar in Cu+Cu collisions at 62 and 200 GeV.

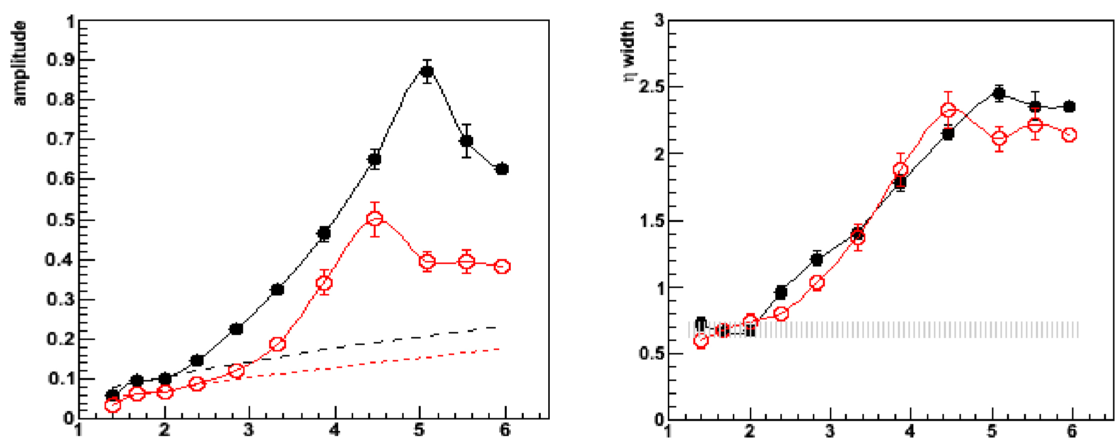

Fig. 5: Amplitude (left panel) and pseudorapidity width (right panel) of 2-D Gaussian fits to the ridge for Au+Au at 200 GeV (black / solid circles) and 62 GeV (red / open circles), as a function of the centrality parameter ν [15] (larger corresponds to smaller impact parameter). The broken lines on the left and the shaded band on the right correspond to Glauber Linear Superposition scaling.

The large extent of the ridge in pseudorapidity can be understood only if the underlying correlation is imparted early in the collision process. Calculations featuring Glasma flux tubes coupled with a flowing sQGP [9] make rather specific predictions related to the onset of the ridge, with a testable dependence on both beam energy and centrality. Ref. [9] implies that the beam energy region of greatest interest should lie between $\sqrt{s_{NN}}$ = 13 GeV and 35 GeV. Studying the energy dependence of the ridge will allow us to test the conjectured relationship between the ridge, Glasma flux tubes, and the formation of strongly interacting quark gluon plasma. The ridge has featured prominently in overviews of the most important RHIC developments and we regard it as a promising analysis topic for an energy scan.

As before, Table 2 provides quantitative details about statistics requirements for the signals discussed in this section. We expect to have ample statistics to pursue all of the above ridge-related studies down to $\sqrt{s_{NN}}$ ~ 17.3 GeV.

(A-4) Local Parity Violation in Strong Interactions

There are still many open questions related to the non-trivial structure of the QCD vacuum. The generation of mass from spontaneous chiral symmetry breaking, and topological solutions (instantons, sphalerons) are relevant to this discussion. *Event-by-event local strong parity violation* would be highly important new evidence that would lend support to current theoretical understanding, and would have an immediate impact, not just on relativistic heavy ion physics, but on all spheres of physics touched by QCD (high energy physics, cosmology, etc.)

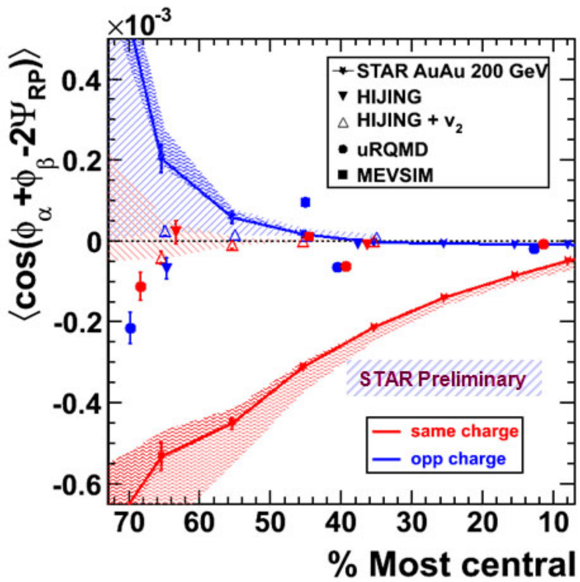

Fig. 6: Centrality dependence of the parity violation signal for Au+Au at 200 GeV. The shaded regions indicate systematic uncertainties, and such uncertainties will be smaller when the analysis is repeated at lower energies.

The observation of a local parity-violating signal assumes the following chain of circumstances. In non-central heavy-ion collisions, a large orbital angular momentum vector (***L***) exists at 90° to the reaction plane, leading to a very intense localized magnetic field (due to the net charge of the system). If the system is deconfined, there can be strong parity-violating domains, and different numbers of left- and right-hand quarks, leading to preferential emission of like-sign charged particles along ***L***. In the azimuthally anisotropic emission of particles,

$$\frac{dN_\pm}{d\phi} \propto 1 + 2a_\pm \sin(\phi - \Psi_{RP}) + \ldots$$

the coefficient a represents the size of the parity-violating signal, and the remaining terms (not shown explicitly) are the familiar ones with coefficients v_n for directed and elliptic flow, etc. However, the coefficient a averages to zero when integrated over many parity-violating domains in many events. If parity violation takes place, a non-zero average signal can be obtained by forming a correlation between pairs of emitted particles (azimuths ϕ_α and ϕ_β) relative to the reaction plane (azimuth Ψ_{RP}), as plotted on the vertical axis of Fig. 6. The observed results [10] are consistent with the expected signal for parity violation, especially the centrality dependence, as seen in Fig. 6. There are caveats attached to this observation – the expected parity violation is parity-odd, whereas the only accessible observable to measure it is parity-even, which means that effects not related to parity violation (e.g., jets and resonances) can contribute to the measured signal [10]. So far, there is no known background, or effect predicted by existing event-generating models, that could account for the observed signals. The shaded regions in Fig. 6 illustrate the limited extent to which background effects could contribute.

There are two separate ways in which the Beam Energy Scan is highly relevant in discussion of local strong parity violation. First, the violation is generally accepted as needing deconfinement to happen. So apart from its very high intrinsic importance, with implications well beyond heavy ion physics, parity violation is a deconfinement signal that we expect to turn-off at some point if we go down low enough in energy. Second is the aspect of how the parity-violating signal and background effects might behave as we scan down in beam energy. Simulations of backgrounds suggest that if the signal survives after the analysis has been repeated over a range of beam energies, the argument that background effects cannot explain it will be even more compelling.

As documented in Table 2, this study of local strong parity violation needs about 5 million events at each BES energy, and thus our run plan will allow this study to be pursued at all energies down to 7.7 GeV. These measurements illustrate a unique capability offered by STAR's large acceptance: multi-dimensional imaging of correlations and fluctuations give better insight into the source and nature of observed signals.

B. Search for Phase Transition and a Critical Point

(B-1) Elliptic and Directed Flow

For collision energies that result in trajectories that cross the 1st-order phase transition region, there is expected to be a significant softening of the equation of state. Thus signatures of the 1st-order phase transition will be found in the hydrodynamic evolution of the phase-space distribution.

Elliptic flow (v_2) has been studied at RHIC, SPS, AGS, and lower energies. The most extensive energy systematic is p_T integrated and for unidentified particles, as shown in Fig. 7. At energies below $\sqrt{s_{NN}}$ = 3.8 GeV, the elliptic flow is negative (out-of-plane). This is interpreted as a squeeze-out due to the interaction between the spectators and the participant zone [11]. Ideal hydrodynamics had predicted a non-montonic dependence of v_2 with collision energy due to the softening near T_c [12], however, this has not been seen in this general study; above 3.8 GeV, the elliptic flow becomes positive and increases with collision energy. In order to remove the effects of the initial conditions, v_2/ε (where ε is the initial state eccentricity) has been studied as a function of centrality for RHIC energies and compared to hydrodynamic predictions [13]. It is only at the highest particle densities that the systems seem to approach the ideal hydro limits [14].

Measuring v_2 with a selection on transverse momentum is important for at least two reasons. Firstly, comparison with any model should only be done within the range of validity of that model. Hydrodynamics is typically assumed to be valid below 1.5 GeV/c [12], and the shape of the p_T-dependence of v_2 is a good indication of when viscous effects dominate. Secondly, it has recently been stressed [51] that focus on some specific range in p_T can generate apparently-exciting but actually-trivial artifacts in the excitation function of v_2. In addition to p_T selection, it is crucial to have good particle identification, for two important reasons. Firstly, several authors [53,54] have pointed out the much stronger sensitivity on the EOS for particles much heavier than the pions, which dominate inclusive charged particle measurements. For example, a potential signature of the phase transition is the collapse of proton elliptic flow [46]. NA49 had made an initial report of an observation of this effect in $\sqrt{s_{NN}}$ = 8.77 GeV data [17], however, more precise results and more detailed comparisons to the theoretical models are needed in order to draw firm conclusions. Secondly, the defining characteristic of collectivity in hydrodynamical scenarios is the interplay of the velocity field with thermal motion; this gives rise to an unavoidable and characteristic mass scaling of spectra and v_2. The observation of this scaling signals that hydro concepts may be applied, whereas its breakdown suggests strong viscous corrections, or particle-dependent mechanisms such as quark coalescence or particles escaping early from the collision (e.g. phi meson).

The directed flow (v_1) is generated during the nuclear passage time, T_{pass}, and therefore it can probe the onset of the bulk collective dynamics as long as this passage time is greater than the time required to achieve thermalization, τ_0. The nuclear passage time can be estimated as $T_{pass}=2R/\gamma$, which varies from ~ 5.6 fm/c for $\sqrt{s_{NN}}$ = 5 GeV to ~ 0.35 fm/c for $\sqrt{s_{NN}}$ = 39 GeV; the timescale for thermalization is expected to be proportional to $(dN/dy)^{-1/2}$ and varies from ~ 1.2 fm/c for $\sqrt{s_{NN}}$ = 5 GeV to ~ 0.7 fm/c for $\sqrt{s_{NN}}$ = 39 GeV ($T_{pass} > \tau_0$ for all collision energies proposed in Table 1 except 39 GeV). The shape of v_1 vs. rapidity is of special interest because it has been identified as a key phase transition signature [18]. At low energies, the v_1 is almost directly proportional to the rapidity. In the energy range proposed in Table 1, the directed flow is predicted to be near zero and to even exhibit a characteristic "*wiggle*". In Fig. 8, we show suggestive preliminary results of a v_1 analysis of 9.2 GeV test run data.

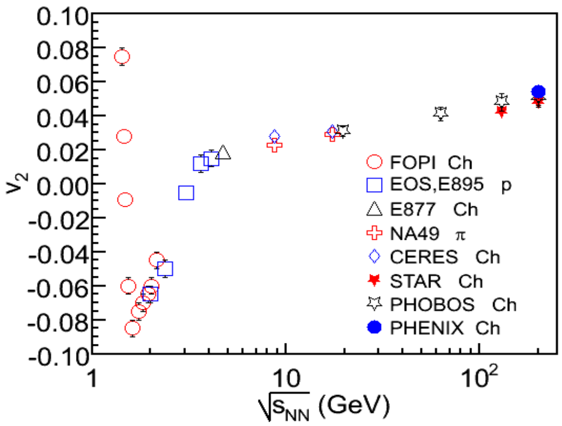

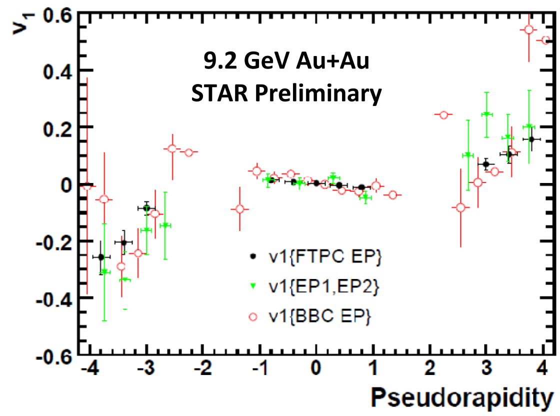

Fig. 7: The charged particle v_2 collision energy excitation function shows a change from out-of-plane to in-plane.

Fig. 8: A "*wiggle*" in v_1 near $y = 0$ is a promising phase transition signature; however it is important to distinguish pion from proton v_1, which the full ToF will allow.

(B-2) Azimuthally Sensitive HBT

Momentum-space correlations tell only half of the story of the hydrodynamic evolution. HBT radii measured relative to the event plane are the coordinate-space analogs of directed and elliptic flow [19, 20], and are expected to be sensitive to a softening in the EOS related to a 1st-order phase transition [21].
STAR has measured the azimuthal dependence of the π HBT radii with respect to the reaction plane [22]. In addition to the overall size of the source, this analysis reveals the transverse *shape* (described by the eccentricity, $\varepsilon = (\sigma_y^2 - \sigma_x^2)/(\sigma_y^2 + \sigma_x^2)$, where σ_x^2 is the in-plane axis, and σ_y^2 is the out-of-plane axis). The shape is found to be extended out-of-plane at freeze-out. Quantitatively, however, it has a lower eccentricity, reflecting dynamic evolution of the system.

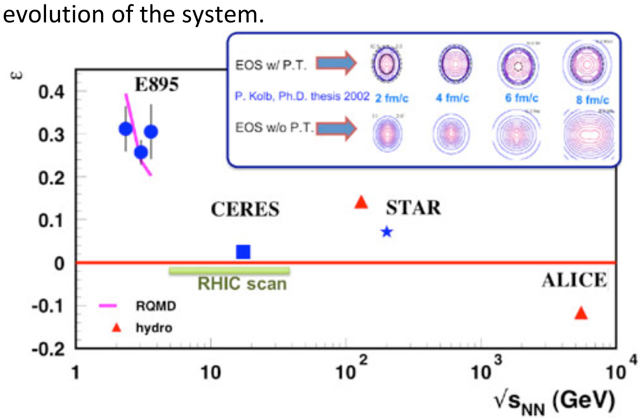

Fig. 9: Freeze-out anisotropy from 2nd -order oscillations of HBT radii. All measurements are subject to ~30% systematic uncertainty. Inset shows hydro evolution of source shape for an equation of state with (upper) and without (lower) softening due to finite latent heat. [25]

The eccentricity has been measured at a few lower energies, as well. Since the lifetime of the system and the elliptic flow increase with collision energy, one naively expects that the freeze-out shape becomes less out-of-plane extended, and may even become in-plane extended (as predicted [21] for example at the LHC). However, Fig. 9 shows instead an intriguing non-monotonic behavior. A possible explanation may be that at low energies the stiff EOS of a hadronic system generates a large pressure, pushing the system towards a round shape ($\varepsilon = 0$). At some energy, a threshold required to generate a phase transition is crossed. This generates a "soft point" in the EOS, and the push towards a round state is reduced. At still higher energies, the stiff EOS of the QGP phase leads again to a decreasing eccentricity with increasing $\sqrt{s_{\mathrm{NN}}}$.

This would be the direct analog of the non-monotonic excitation function of v_2 originally predicted by ideal hydro models with a softening due to a phase transition [12, 23]. The signal in v_2 has not been observed. However, the spatial anisotropy probed by HBT is weighted in the time evolution differently, so may retain sensitivity to the softest point. In any event, Fig. 9 represents one of the very rare bulk-sector probes with an unexplained non-monotonic excitation function, demanding further exploration.
The 3-dimensional shape of the spatial configuration approximates a tri-axial ellipsoid. One can extract the angle between its major axis and the beam direction. This "*tilt angle*" [20] is the spatial analog of the "*flow angle*" [24]

formerly used to characterize directed flow. Simultaneous measurement of both the tilt angle and v_1 provides unique insight into the nature and physics of directed flow at lower energies. As discussed above, crossing a threshold to a phase transition will generate a "wiggle" in the directed flow at midrapidity. This same physical scenario is predicted to generate a non-trivial fingerprint [25] of the coordinate-space configuration. The geometry will probe the physics *behind* the "third component" of flow generating the v_1 wiggle.

(B-3) Fluctuations

The search for a critical point can follow two parallel strategies 1) is to find direct evidence of the divergence of fluctuations expected at the critical point, 2) is to bracket the location of the critical point by finding evidence for a first order phase transition at lower μ_B. It is important to understand the characteristics of the fluctuations and correlations expected in case the system passes through the region near the critical point, or in case it passes through a first order phase transition. Those correlations and fluctuations must be disentangled from backgrounds such as resonance decays, jet fragmentation, elliptic flow, and other sources of correlations not related to the critical point or to clumping due to spinodal phase separation at the hadronization phase boundary [55].

Understanding the origin of the already observed non-statistical correlations and fluctuations [56] requires highly differential information at a variety of centralities. Of particular experimental interest is the longitudinal and azimuthal width of any anomalous correlations and the system size dependence of the associated fluctuations. With particle identification and a large uniform acceptance in $\Delta\eta$ and $\Delta\phi$, STAR provides unprecedented capabilities for these studies. This will allow STAR to disentangle the various sources of correlations and identify those related to a first order phase transition or a critical point. Since they are formed later in the system's evolution, these correlations should be narrow in longitudinal extent, while the azimuthal width will depend on the strength of the radial flow and the temperature of the system. Once backgrounds have been accounted for, the system-size dependence of the correlations can reveal information about the order of the phase transition [57]. In particular, a first order phase transition will lead to a system-size dependence whereas a smooth cross-over will not [58]. Performing these differential correlations and fluctuations analyses at a variety of centralities will require approximately 5 million events per energy.

The characteristic signature of the existence of a critical point is an increase, and divergence, of fluctuations [26]. Lattice QCD calculations [27] indicate large jumps in the baryon, charge, and strangeness susceptibilities as a function temperature of the system; see Fig. 10. These susceptibilities can be related to event-by-event moments of various observables in heavy-ion collisions, in particular to fluctuations of conserved quantities (net charge, net baryon and net strangeness). Theoretical calculations show that the net proton fluctuations, which are experimentally accessible, are a good substitute for net baryon fluctuations [28]. Particle ratios, e.g. K/π and p/π, probe medium dynamics at chemical freeze-out. They are also convenient to study because volume effects are canceled.

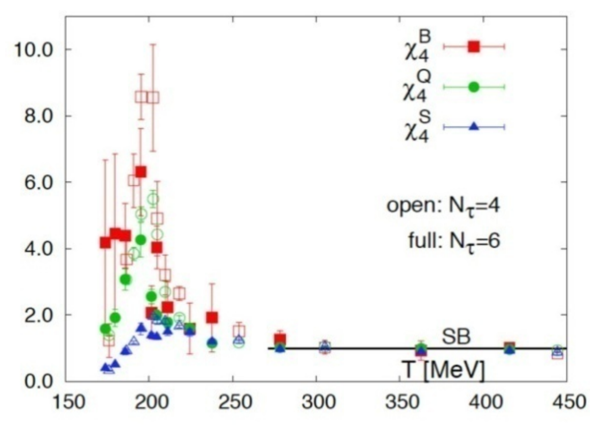

Fig. 10: Quadratic fluctuations of baryon number, electric charge and strangeness. All quantities have been normalized to the corresponding free quark gas values [9].

The fluctuations of momentum of the charged pions are expected to be sensitive to critical fluctuations [29], because pions couple strongly to the fluctuations of the sigma field (the magnitude of the chiral condensate) which is the order parameter of the phase transition, and since the condensate magnitude is predicted to show increased fluctuations in the vicinity of a critical point, these signatures should be imprinted on the pion [29].
Preliminary studies show [30] that they are all within the reach and capabilities of the STAR detector.
<u>K/π fluctuations</u>: The changes in susceptibilities as a function of the temperature illustrated in Fig. 10 might be observable as deviations of fluctuations from a monotonic dependence on incident energy in central collisions.

However, changes in the underlying physics can also induce changes in the fluctuations as a function of incident energy. To gain insights into what might be expected from K/π fluctuations as a function of beam energy, the experimental results were compared to predictions from the UrQMD [31] and the HSD [32] models, as illustrated in Fig. 11. The UrQMD and HSD models reproduce results at RHIC energies, however at lower energies, UrQMD under-predicts the fluctuations, while HSD reproduces the lowest and the highest energies, but over-predicts in the range $\sqrt{s_{NN}}$ = 8-20 GeV. Detailed discussion and comparisons with the AMPT model [33] can be found in Ref. [1]. The fact that all presently-available models have a serious problem with reproducing observed data, combined with the lack of experimental data in the range of $\sqrt{s_{NN}}$ = 20 - 60 GeV, means that the question of non-monotonic behavior of K/π fluctuations must be answered with additional measurements. Of particular interest is the magnitude of K/π fluctuations at the lower end of the proposed energy scan range, as this may shed light on the monotonic vs. non-monotonic behavior of the NA49 "horn". With the proposed run scenario, the fluctuations at 7.7 GeV will be analyzed with adequate statistics, while the proposed number of events for 5 GeV K/π fluctuation analysis may only indicate the trend.

STAR is perfectly suited to perform these measurements. Fig. 12 shows the estimated statistical error for STAR's σ_{dyn} for the charge-integrated K/π ratio with, and without, ToF information. The measurements were assumed to be based on only 100k central events. Also shown, for comparison, are the current NA49 and STAR measured data points. With the ToF, STAR's relative error is ~ 5%, and without the ToF, this doubles to ~10%. To make these measurements, one needs to attempt to measure all the kaon and pions. The K reconstruction efficiency as a function of p_T is rather low, mainly due to kaon decays. STAR's ToF will extend the clean PID range to higher p_T and thus gain essential coverage. As already mentioned, not only coverage, but clean PID is needed. The ToF plays an essential role in eliminating electron contamination at low p_T.

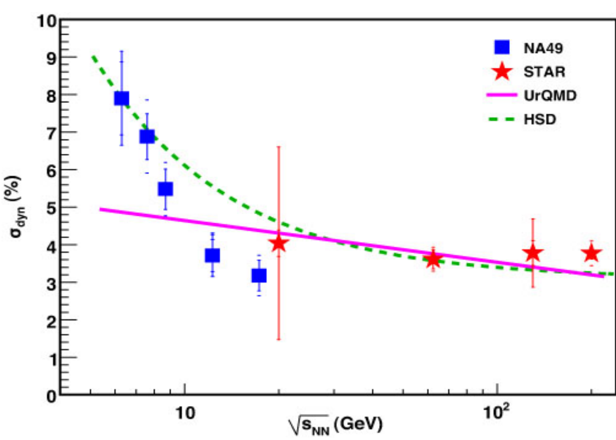

Fig. 11: Comparison of the predictions of the HSD and UrQMD models to the experimental data for σ_{dyn} for K/π. Lines are drawn to guide the eye.

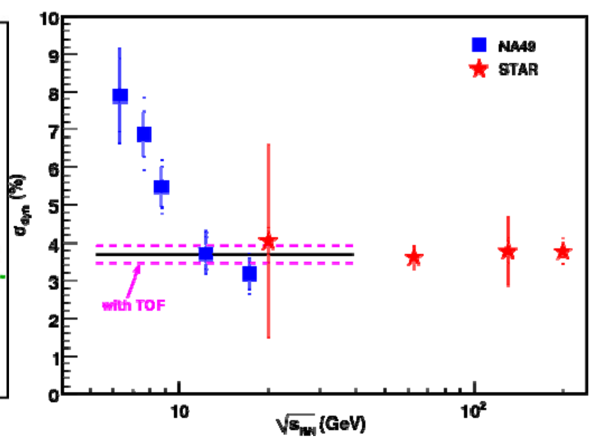

Fig. 12: Estimate of the error in σ_{dyn} for charge-integrated K/π fluctuations, based on 100K central events analyzed in the STAR detector (with the newly completed ToF). Shown for comparison are the current measurements from NA49 and STAR.

p/π fluctuations: The study of p/π fluctuations may provide information about baryon fluctuations. The quadratic baryon susceptibilities show a marked peak at temperatures near the critical temperature (see Fig. 10). p/π fluctuations have been studied as a function $\sqrt{s_{NN}}$ by NA49 [34] and by STAR at the same energies as used to study K/π fluctuations. Results were compared to UrQMD and AMPT models. Both models are reasonably close to the experimental data. And again, like in the case of K/π, there is a gap in experimental information at lower energies, which needs to be remedied with new data.

<p_T> fluctuations: Average transverse momentum fluctuations are discussed in the literature in the context of a search for the QCD critical point [29], [35]. It is expected that close to the critical point, long-range correlations are very strong, resulting in enhanced momentum fluctuations, especially for small momenta (small p_T values are important because correlation length r diverges at the Critical Point and $\Delta r\, \Delta p \sim h/2\pi$). The signature in this case would be a maximum in the excitation function of < p_T>-fluctuations at the energy corresponding to the location of the critical point. In addition to the transverse momentum fluctuations for all charged particles, one can investigate p_T fluctuations of the negative and positive charges independently, as well as the cross-correlations between them [36].

Measurements of $\langle p_T \rangle$ fluctuations are extremely challenging if the experiment does not have 2π acceptance, because there are a number of effects that can compromise the strength of the signal and are not fully correctable without 2π coverage (for instance elliptic flow can cause a non-statistical fluctuation of the $\langle p_T \rangle$ if the experiment does not have 2π acceptance). This is not a concern for the STAR detector, which has full azimuthal symmetry. STAR analyzed successfully those fluctuations in Au+Au collisions at energies from 20 to 200 GeV. The $\langle p_T \rangle$ was measured for all events and also estimated for mixed events. The results were compared, and a difference between the data and mixed events was interpreted as an indication of non-statistical fluctuations; see an example in Fig. 13. Current results show significant non-statistical fluctuations at all energies measured by STAR [37]. $\langle p_T \rangle$ fluctuations have been also investigated at the CERN SPS (CERES [38] and NA49 [39] experiments). Together these measurements cover a wide range of beam energies. The compilation of all $\langle p_T \rangle$-fluctuation measurements is shown in Fig. 14 (the variable Σp_T represents the dynamical contribution to event-by-event $\langle p_T \rangle$ fluctuations in units of the overall average $\langle p_T \rangle$ [49,50]).The fluctuations are of the order of 1% of $\langle p_T \rangle$ in all cases, and show virtually no beam-energy dependence.

Currently there are no measurements with full azimuthal coverage in collider geometry below $\sqrt{s_{NN}}$ = 20 GeV where, most probably, the CP is located. This fact, together with a relatively large gap in the measurements between 20 and 60 GeV, does not yet allow us to draw conclusions regarding non-statistical fluctuations, their magnitude and nature, and possible relation to the critical point. The BES program, particularly the part of the scan below injection energy, will allow us to clarify the situation. It is important to stress that all measurements will be done with the same apparatus, and therefore, with the same systematics.

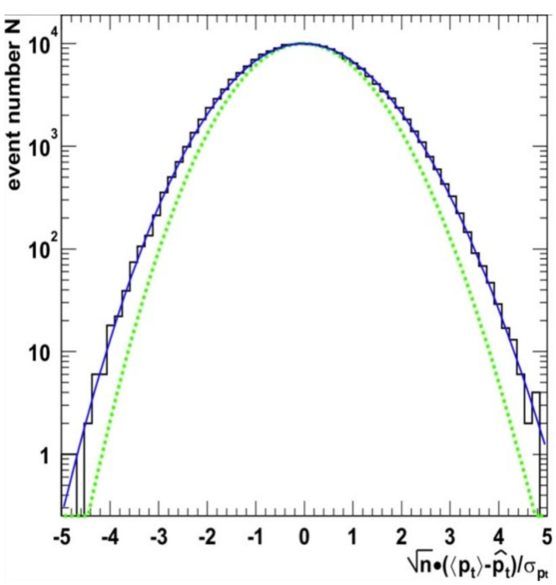

Fig. 13: The measured $\langle p_T \rangle$ in Au+Au collisions at 200 GeV (solid histogram), and from event mixing (green curve). The fit to the data is shown as the blue curve.

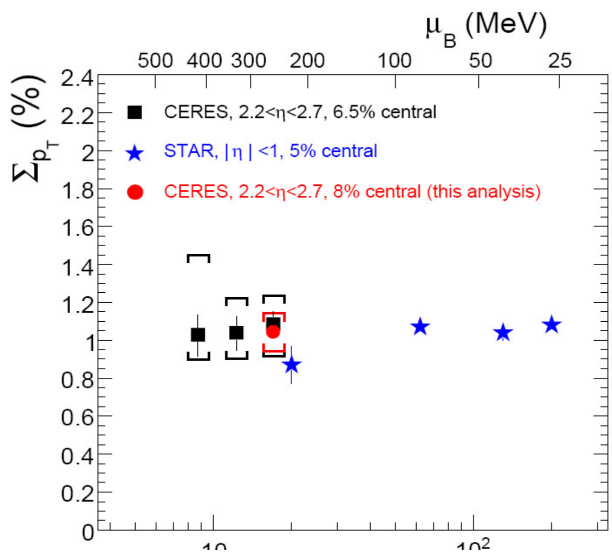

Fig. 14: Normalized dynamical fluctuation observable Σp_T in central Pb+Au and Au+Au collisions for different center of mass energies. The figure is from Ref. [38].

Higher Moments, Kurtosis: To date, most experimental fluctuation measures have concentrated on the second moments (proportional to the square of the correlation length). However, estimates of the magnitude of correlation length in heavy-ion collisions indicate it could be small around the critical point (of the order of 2-3 fm) [40], making it challenging to be detected in experiments. It has been proposed that higher moments of event-by-event pion and proton multiplicities are significantly more sensitive to the existence of the critical point compared to measures based on second moments. The fourth moment, the kurtosis, of these multiplicity distributions is expected to be proportional to the seventh power of the correlation length [40]. In addition, it is expected that the evolution of fluctuations from the critical point to the freeze-out point may lead to a non-Gaussian shape in the event-by-event multiplicity distributions. Due to the above reasons, the kurtosis of multiplicity distributions would then provide a more sensitive observable for the search of the QCD critical point. Further in lattice calculations, which assume the system to be in thermal equilibrium, the kurtosis of event-by-event net-baryon number, net-charge and net-strangeness are related to the respective susceptibilities. These susceptibilities show large values or diverge at the critical temperature in presence of a QCD critical point [26, 27, 40, 41]. The measurement of higher moments of event-by-event identified particle multiplicity distributions will provide a direct connection between experimental observables and Lattice Gauge Theory calculations [40]. Note that the ratio of the fourth and second moments (Fig. 15) not only provides a strong signal but also is particularly convenient from the experimental point of view, because all unknown volume terms cancel out.

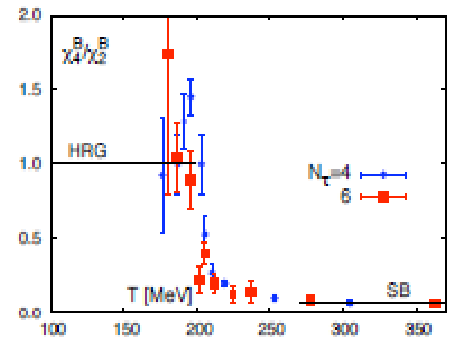

Fig. 15: The ratio of the fourth and second order cumulants of baryon number as a function of temperature. The value from the hadron gas model (HRG) is for the temperature range from100 to 200 MeV

Using STAR's large acceptance and excellent PID capabilities at mid-rapidity, protons and anti-protons can be cleanly identified. One can therefore carry out both net-charge and net-proton kurtosis analyses, as motivated by lattice QCD calculations.
Statistics of the order of 5M events at each energy point across the energy range from 7.7 GeV and up will allow a net proton kurtosis analysis with an uncertainty of 0.1 [42].

Flexibility of STAR and Readiness for Unanticipated Observations

The energy range of the BES program at RHIC covers the span of most available Lattice QCD estimates of the location of the critical point. It will span from the second-order cross-over regime, past the location of the critical point in several estimates, and into the region dominated by the first-order transition (T, μ_B) ~ (170-100 MeV, 20-500 MeV). The experiments must be capable of making comprehensive measurements of all the signals related to critical phenomena and the evolution with beam energy of unusual medium properties attributed to the new state of matter already studied at the upper RHIC energies (how they vary and, eventually, disappear). And, of course, all experimenters must be open to new surprises in unexplored regions, and should have the most flexible tools for investigating any unforeseen discoveries.
While the energy scan program at the CERN SPS (with beams from 20 to 158 GeV/c in fixed target mode, equivalent to $\sqrt{s_{NN}}$ = 6.3 – 17.3 GeV) reported interesting phenomena with possible relevance to a phase transition, the evidence remains inconclusive [43]. With the BES program at RHIC, we expect to greatly expand the scope and range of relevant measurements, and thus bring much improved clarity to the situation. Using a collider for energy scan studies brings two tremendous advantages over a fixed-target facility:

(1) The phase space covered by the detectors in collider experiments changes very little with beam energy. In fixed target experiments, the detector acceptance changes significantly with energy and in order to understand how the

underlying physics evolves with beam energy, extrapolation to a common phase space is necessary. This process is based on assumptions and therefore introduces additional systematic uncertainties.
(2) Track density at mid-rapidity varies very slowly with energy for collider geometry, while it increases dramatically with energy in fixed-target experiments. This results in increased technical difficulties in tracking (e.g. changes in hit sharing and track merging, changes in *dE/dx* and momentum resolution). When going down to lower beam energy from 200 GeV, due to the low multiplicity and luminosity, the STAR TPC will perform slightly better in terms of efficiency and other performance parameters.

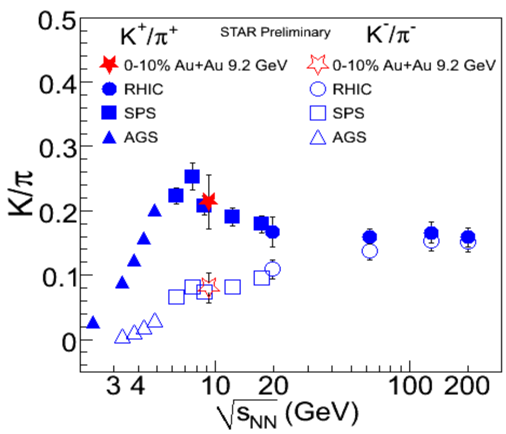

Fig. 16: The K/π ratio as a function of beam energy. The STAR 9.2 GeV test data are shown in comparison to world data. The error bars for the 9.2 GeV result is dominated by statistical errors.

The STAR detector, due to its large and uniform acceptance and excellent particle identification capabilities (enhanced by the completed Time of Flight barrel in 2010), is uniquely positioned to carry out this program in unprecedented depth and detail.
The STAR experiment already has a proven performance record and significant experience with low energy running. Low energy runs were taken with 19.6 GeV Au+Au collisions in 2001 and 22.4 GeV Cu+Cu in 2004. During a brief machine development test in 2008, the STAR detector successfully took data (about three thousand good events) at $\sqrt{s_{NN}}$ = 9.2 GeV. All systems performed well, and as an example of physics results from this short test run, Fig. 16 shows a comparison of 9.2 GeV data (marked with the red stars) with data from other experiments at different energies. The K/π ratio vs $\sqrt{s_{NN}}$ measurements are in very good agreement with the rest of the world data. All other STAR measurements at 9.2 GeV [44] are also consistent with those reported by earlier experiments. We are confident that STAR's capability over the proposed energy scan region is fully understood, and we are ready for the proposed run.

STAR Run Plan for First Energy Scan

The BES program is planned in at least two stages. For the first BES run (RHIC Run-10) we propose to run a wide range of energies, from $\sqrt{s_{NN}}$ =7.7 to 39 GeV (see Tables 1 and 2) with an additional 200 k events at 5 GeV for measurement of K/π fluctuations (nominally utilizing a machine development test at that energy). We have selected lower $\sqrt{s_{NN}}$ values that give the greatest discovery potential for the critical point, as well as higher energies to cover the current gap between RHIC and the SPS. We have chosen energy steps spaced uniformly between top SPS energies and RHIC's 62.4 GeV.
It is highly preferable for the first run to take place in 2010 prior to the beam pipe change in STAR and PHENIX, and prior to removal of FTPCs in STAR. The new 4-cm diameter beam pipe may seriously complicate successful running at sub-injection energies due to increased transverse size of the beams below injection energy [45]. The STAR FTPCs play an important role in providing information about the 1st-order event plane as well as extending pseudorapidity coverage out to 4 units on each side.
Data from the 9.2 GeV Au+Au test run allowed us to estimate the actual rate of triggered events within a useable range of vertex positions. The test run was very short with emphasis on demonstrating capability rather than tuning for the highest possible event rate. BNL Collider Accelerator Division (C-AD) staff have indicated a high degree of confidence that these rates can be increased by a factor of about 6 via improvements in injection efficiency and by increasing the number of bunches in the machine. Additional tuning is likely to provide further incremental rate improvements. Another option being explored is continuous injection to fill the bunches and extend the beam lifetime. This is expected to increase the integrated rate by a factor of about 2. To be very conservative, none of these further possible enhancements are included in the event rate estimates presented Table 1 and 2. Based on consultation with C-AD, it is estimated that the rates will scale according to γ^3 up to injection energy and by roughly γ^2 above that. These estimates were cross-checked against actual data rates taken by STAR during the early injection-energy run and also against measurements of the injection energy luminosity

Beam Energy	Event Rate	8-hr Days/ 1M Events	Events proposed	8-hr days proposed
5	**0.8**	**45**	**100 k**	**5**
7.7	**3**	**11**	**5 M**	**56**
11.5	**10**	**3.7**	**5M**	**19**
17.3	**33**	**1.1**	**15M**	**16**
27	**92**	**0.4**	**33M**	**12**
39	**190**	**0.2**	**24M**	**5**

Table 1: The proposed run duration at each energy is determined by the number of Minimum Bias events needed to perform the detailed measurements discussed in the previous sections; see Table 2.

	Collision Energies (GeV)	**5**	**7.7**	**11.5**	**17.3**	**27**	**39**
Section	Observables	Millions of Events Needed					
A1	n_q scaling π/K/p/Λ $(m_T\text{-}m_0)/n$<2GeV	8.5	**6**	**5**	**5**	**4.5**	**4.5**
A1	ϕ/Ω up to p_T/n_q=2 GeV/c		56	25	**18**	**13**	**12**
A2	R_{CP} up to p_T ~4.5 GeV/c (at 17.3) 5.5 (at 27) & 6 GeV/c (at 39)				**15**	**33**	**24**
A3	untriggered ridge correlations		27	13	**8**	**6**	**6**
A4	parity violation		**5**	**5**	**5**	**5**	**5**
B1	v_2 (up to ~1.5 GeV/c)	**0.3**	**0.2**	**0.1**	**0.1**	**0.1**	**0.1**
B1	v_1	0.5	**0.5**	**0.5**	**0.5**	**0.5**	**0.5**
B2	Azimuthally sensitive HBT	4	**4**	**3.5**	**3.5**	**3**	**3**
B3	PID fluctuations (K/π)	1	**1**	**1**	**1**	**1**	**1**
B3	net-proton kurtosis	5	**5**	**5**	**5**	**5**	**5**
B3	differential corr & fluct vs. centrality	5	**5**	**5**	**5**	**5**	**5**
B3	integrated p_T fluct (T fluct)						
See[1]:	charge-photon fluctuations (DCC)	1	**1**	**1**	**1**	**1**	**1**
	kink/step/horn	**0.1**	**0.1**	**0.1**	**0.1**	**0.1**	**0.1**
	v_2 fluctuations	0.5	**0.5**	**0.5**	**0.5**	**0.5**	**0.5**
	HBT (R_l, R_o/R_s)	0.8	**0.8**	**0.5**	**0.5**	**0.5**	**0.5**
	Jet/ridge 2<trig<4, 1<assoc<trig				30	**8.8**	**4.5**
	Jet/ridge 3<trig<6, 1.5<assoc<trig					53	**24**
	Baryon-Strangeness cor (hypernuc)						50
	Forward π^- yield (rapidity scaling)						
	Forw. $\gamma(\pi^0)$ yield (rapidity scaling)						
	Long-range forward-backward corr.						
	Other PID fluctuations (esp. K/p)						
	Particle ratios (many examples)						
	p_T spectra						
	Prod. of light nuclei & antinuclei						
	Yields of species & stat model fits						

Table 2: Observables and statistics needed for the first BES run. The observables in the yellow-shaded area relate to the search for turn-off of new phenomena already established at higher RHIC energies (see section A), while observables in the blue-shaded area search for a phase transition or critical point (see section B). The numbers listed in boldface above are all within reach (nominally require no more than 1.5 times the proposed statistics) in the first BES run plan as set out in Table 1. The remaining numbers (not boldface) will need to wait for higher statistics in a subsequent run. The white part above is briefly introduced in this document, and is explained in detail in Ref. [1].

under current operating conditions. Results are found to be consistent [1]. From these estimated event rates, and assuming that we take data for an average of 8 hours per day of beam, we determine the number of days necessary to acquire one million events at each of the proposed energies, as shown in Table 1. Note that all estimates in Tables 1 and 2 already allow for detector acceptance and vertex position cuts.

The observables listed in the white part of Table 2 are not considered at the present moment to be highest priority analyses that determine the structure of our overall run plan for RHIC Run-10, but nonetheless are priorities for individual groups within the STAR collaboration and will definitely be carried out as per the details discussed in Ref. [1]. If the past history of heavy-ion physics is any guide, the most striking and unexpected discoveries of the BES program may well emerge from the analyses listed in this white area of Table 2, and we consider STAR's greatest strength to be its ability, through flexibility and broad acceptance, to make serendipitous discoveries.

The lower beam energies are specifically chosen to map out a region around the "horn" in the K/π ratio observed by SPS experiments [40]. All the selected energies allow collisions at both STAR and PHENIX. After analysis of the first BES run, we propose that a second scan be performed, probably focused more specifically on a few collision energies. These energies and physics topics will be chosen to explore in more depth the most interesting regions found via the first scan. We argue that the most important energy region for the physics of the BES program is the lower end of the proposed energy span, and therefore we propose to start the energy scan at 7.7 GeV. After about two weeks of data taking, we will be able to evaluate the correctness of the estimates provided in Tables 1 and 2 of this document, and possibly adjust the duration of the run, if needed. At the time of writing, to the best of our knowledge, we will require 5 M events at 7.7 GeV. We expect that the second run, with more data at fewer energies, will take advantage of further luminosity upgrades proposed by BNL C-AD.

References

[1] Long BES document - in preparation.

[2] J. Adams *et al.*, Nucl. Phys. A **757**, 102 (2005); also whitepapers from the other three RHIC experiments.

[3] F.R. Brown *et al.*, Phys. Rev. Lett. **65**, 2491 (1990).

[4] M. Asakawa and K. Yazaki, Nucl. Phys. A**504**, 668 (1989); A. Barducci *et al.*, Phys. Lett. B **231**, 463 (1989), Phys. Rev. D**41**, 1610 (1990), Phys. Rev. D**49**, 426 (1994); J. Berges and K. Rajagopal, Nucl. Phys. B **538**, 215 (1999), M.A. Halasz *et al.*, Phys. Rev. D**58**, 096007 (1998); Y. Hatta and T. Ikeda, Phys. Rev. D **67**, 014028 (2003).

[5] M.A. Stephanov, Prog. Theor. Phys. Suppl. **153**, 139 (2004) [Int. J. Mod. Phys. A **20**, 4387 (2005)].

[6] M. Asakawa *et al*., Phys. Rev. Lett. **101**, 122302 (2008).

[7] For a recent review of the topic of multifragmentation and the liquid-vapor phase transition, providing many insights into the general topic of phase transitions in small systems, see B. Borderie and M.F. Rivet, e-print arXiv:0812.3524 (and references therein).

[8] C. Blume *et al*. (NA49 collaboration), J. Phys. G. Nucl. Part. Phys. **35,** 044004 (2008).

[9] A. Dumitru, F. Gelis, L. McLerran, and R. Venugopalan, Nucl. Phys. A **810**, 91 (2008); P. Sorensen, arXiv: 0811.2959

[10] S.A. Voloshin *et al*., (STAR collaboration), e-print arXiv: 0806.0029 and B.I. Abelev *et al*., (STAR collaboration), e-print arXiv: 0906.----.

[11] H. Sorge, Phys. Rev. Lett. **78**, 2309 (1997), nucl-th/9610026.

[12] P.F. Kolb, J. Sollfrank, and U.W. Heinz, Phys. Rev. C **62**, 054909 (2000).

[13] S.A. Voloshin, A.M. Poskanzer, and R. Snellings, arXiv: nucl-ex/0809.2949.

[14] T. Hirano *et al.*, J. Phys. G **34,** S879 (2007).

[15] M. Daugherity *et al.* (STAR collaboration), J. Phys. G **35**, 104090 (2008).

[16] (PHENIX), Phys. Rev. Lett. **94**, 232302 (2005); R. Lacey *et al.*, arXiv: nucl-ex/0708.3512.

[17] C. Alt *et al.* (NA49 collaboration), Phys. Rev. C **68**, 034903 (2003), nucl-ex/0303001.

[18] R. Snellings *et al.,* Phys. Rev. Lett. **84**, 2803-2805 (2000); J. Brachmann *et al.*, Phys. Rev. C **61**, 024909 (2000), nucl-th/9908010; L. P. Csernai and D. Rohrich, Phys. Lett. B **458**, 454 (1999), nucl-th/9908034; H. Stoecker, Nucl. Phys. A **750**, 121 (2005).

[19] F. Retiere and M.A. Lisa, Phys. Rev. C **70,** 044907 (2004) .

[20] M.A. Lisa, U. Heinz, U. Wiedemann, Phys. Lett. B **489**, 287 (2000).

[21] U. Heinz and P. Kolb, Phys. Lett. B **542,** 216 (2002).

[22] J. Adams *et al.* (STAR), Phys. Rev. Lett. **93,** 12301 (2004).

[23] U. Heinz and P. Kolb, Phys. Lett. B **459**, 667 (1999).
[24] M. Gyulassy, K.A. Frankel and H. Stoecker, Phys. Lett. B **110**, 185 (1982); W. Reisdorf and H.G. Ritter, Ann. Rev. Nucl. Part. Sci. **47,** 663 (1997).
[25] M.A. Lisa and S. Pratt, arXiv: 0811.1352.
[26] V. Koch, e-print arXiv: 0810.2520.
[27] M. Cheng *et al.*, e-print arXiv: 0811.1006.
[28] Y. Hatta, M. Stepanov, Phys. Rev. Lett. **91**, 102003 (2003).
[29] M. Stepanov, K. Rojagopal, E.V. Shuryak, Phys. Rev. D**60** 114028 (1999), hep-ph/9903292.
[30] J. Adams *et al*., (STAR collaboration) Phys. Rev. C **72**, 044902 (2005).
[31] M. Bleicher *et al*., J. Phys. G **25**, 1859 (1999).
[32] M.I. Gorenstein *et al.*, e-print arXiv: 0811.3089.
[33] Z.-W. Lin *et al*., Phys. Rev. C **72**, 064901 (2005).
[34] C. Alt *et al*., (NA49 collaboration) e-print arXiv: 0808.1237.
[35] M. Stepanov, K. Rojagopol, E.V. Shuryak, Phys. Rev. Lett. **81** 4816 (1998), hep-ph/9806219.
[36] S. Jeon, V. Koch, "Event-by-event fluctuations" in *Quark Gluon Plasma 3*, R. Hwa, X. Wang eds., p. 430, World Scientific, Singapore, 2004.
[37] J. Adams *et al*., (STAR Collaboration), PRC 71, 044902 (2005).
[38] D. Adamova *et al*., (CERES Collaboration), Nucl. Phys. A **811**, 179 (2008).
[39] H. Appelshauser *et al*., (NA49 Collaboration), Phys. Lett. B **459**, 679 (1999); M. Rybczynski *et al*., (NA49 Collaboration), nucl-ex/0805.2245
[40] M.A. Stepanov, e-print arXiv: 0809.3450.
[41] R.V. Gavai and S. Gupta, Phys. Rev. D **71**, 114014 (2005).
[42] T. Schuster *et al.*, e-print arXiv: 0903.2911.
[43] S.V. Afanasiev *et al*., (NA49 Collaboration), Phys. Rev. C **66**, 054902 (2002); C. Alt *et al*., (NA49 Collaboration), Phys. Rev. C **68**, 034903 (2003); C. Roland *et al*., (NA49 Collaboration), J. Phys. G **30**, S1381 (2004).
[44] L. Kumar *et al.* (STAR collaboration), SQM 2008, QM 2009.
[45] C-AD communication.
[46] For an overview, see H. Stoecker, arXiv:0710.5089, published in PoS CPOD07:025, 2007.
[47] C. Alt *et al*., (NA49 Collaboration), Phys. Rev. C **77**, 034906 (2008).
[48] M.M. Aggarwal *et al*., (WA 98 Collaboration), Phys. Rev. Lett. **100**, 242301 (2008).
[49] D. Adamova *et al*., (CERES Collaboration), Nucl. Phys. A **727**, 97 (2003).
[50] J. Adams *et al*., (STAR Collaboration), Phys. Rev. C **72**, 044902 (2005).
[51] U. Heinz, QM 2009.
[52] B.I. Abelev *et al*., (STAR Collaboration), Phys. Rev. Lett. **99**, 112301 (2007); J. Adams *et al*., (STAR Collaboration), Phys. Rev. Lett. **95**, 122301 (2005).
[53] P. Huovinen, Nucl. Phys. A**761**, 296 (2005).
[54] P. Huovinen, P. Kolb, U. Heinz, P.V. Ruuskanen, S.A. Voloshin, Phys. Lett. B **503**, 58 (2001).
[55] J. Randrup, arXiv:nucl-th/0406031.
[56] B.I. Abelev *et al*., (STAR Collaboration), arXiv:0901.1795.
[57] L.F. Palhares, E.S. Fraga and T. Kodama, arXiv:0904.4830.
[58] Y. Aoki, G. Endrodi, Z. Fodor, S.D. Katz and K.K. Szabo, Nature **443**, 675 (2006) [arXiv:hep-lat/0611014]